

Binding and Diffusion of a Si Adatom on the Si(100) Surface

G. Brocks and P. J. Kelly

Philips Research Laboratories, 5600 JA Eindhoven, The Netherlands

R. Car

International School for Advanced Studies, Trieste, Italy

(Received 31 August 1990)

The binding sites for adsorption of a single Si atom on the reconstructed Si(100) surface are identified using first-principles total-energy calculations. We establish several saddle points for the migration of the adatom by mapping out the total energy as a function of its position on the surface. For diffusion parallel to the dimer rows on the surface, we find an activation energy of 0.6 eV; for diffusion perpendicular to the rows, the activation energy is 1.0 eV. One-dimensional hopping motion of individual adatoms should be observable by scanning tunneling microscopy at moderately low temperatures.

PACS numbers: 68.35.Fx, 68.35.Bs, 68.45.Ax, 71.25.Cx

One of the outstanding problems in surface physics is the identification of the binding sites for adatoms and the determination of the activation energies for surface diffusion. The structures formed after deposition of Si on the Si(100) surface have recently been observed with atomic resolution by means of scanning tunneling microscopy¹⁻³ (STM), giving rise to a discussion of the role of anisotropic surface diffusion. It would be very desirable to be able to interpret the experimental observations using models with realistic atomic binding and diffusion parameters.^{4,5} Even the simplest models which have been used in these studies involve several parameters and available experimental data do not yield these parameters directly. For example, the best estimates of the activation energy for diffusion of Si atoms on the Si(111) surface obtained by fitting experimental data with simple models range from 0.2 to 1.6 eV.⁶ In this paper, we will focus on the first-principles determination of those parameters which determine the diffusion of Si adatoms on the Si(100) surface, and which are of fundamental importance in the growth process.

So far, detailed observations of diffusing atoms have only been made on metal surfaces and have recently attracted much attention.⁷ The structure of semiconductor surfaces is, in general, more complicated than that of metals. One might also expect the behavior of adatoms on semiconductor surfaces to be more complicated. Here, we present results of first-principles calculations which for the first time allow us to identify the binding position and migration barriers of a *single* adatom on a reconstructed semiconductor surface. We have chosen to study a Si adatom on the Si(100) surface. We find that the diffusion of the Si adatom is very anisotropic and we predict that it should be directly observable by STM experiments at temperatures somewhat below room temperature.

By mapping out the total energy as a function of the adatom position (x,y) , an energy surface $E(x,y)$ is ob-

tained. At each position the z coordinate of the adatom and the full relaxation of the substrate atoms is calculated by energy minimization. The minimum total energy defines the binding geometry of the adatom and the substrate. The several saddle points on this energy surface determine the activation barriers for diffusion of the adatom along the Si(100) surface. The calculations are performed within the local-density-functional formalism, using norm-conserving pseudopotentials⁸ and a plane-wave basis set. The pseudopotential, in the representation suggested in Ref. 9, includes s and p nonlocal terms. The Si(100) surface is modeled as a repeated slab, which consists of twelve layers of Si atoms and 9.5 Å of vacuum spacing. Inversion symmetry with respect to the middle of the slab is used to increase the computational efficiency. The adatom plus surface is modeled by taking a periodic arrangement of adatoms on the surface and choosing the resulting surface supercell to be so large that the interaction between adatoms in neighboring cells is negligible. In the calculations to be described, we use a $p(\sqrt{8} \times \sqrt{8})R45^\circ$ surface supercell¹⁰ with a cell parameter of 10.86 Å which contains 8 surface atoms. Figure 1 shows this surface supercell in relation to the underlying Si(100) surface geometry. The unit cell used in the calculations thus contains 98 atoms in total.

The energy surface $E(x,y)$ is mapped out in the following way. The adatom is placed at a number of positions (x,y) on the surface. [The dimer rows on the Si(100) surface are parallel to the y axis, and the direction of the dimerization bond is along the x axis; see Fig. 1.] These positions form an equidistant grid with a spacing between the grid points of 0.96 Å in the x and y directions. Starting with the adatom at 2.4 Å above the surface, at each (x,y) position the total energy is minimized simultaneously with respect to the electronic charge density and the remaining ionic degrees of freedom, i.e., the z coordinate of the adatom and the positions of the substrate atoms. Only the positions of the 16

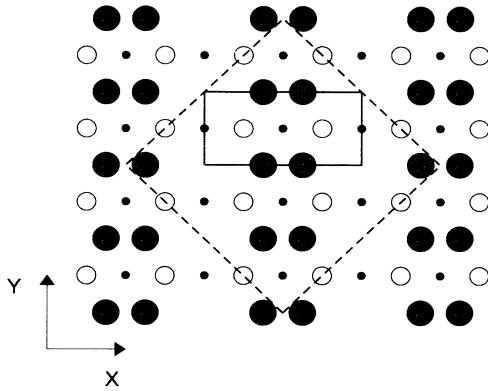


FIG. 1. Projection of the topmost three layers of the $p(2 \times 1)$ -reconstructed Si(100) surface. The large solid circles represent the top-layer atoms, the medium-sized open circles represent the second-layer atoms, and the small solid circles represent the third-layer atoms. The $p(2 \times 1)$ unit cell is indicated by the solid line and the $p(\sqrt{8} \times \sqrt{8})R45^\circ$ unit cell (Ref. 10) by the dashed line.

atoms of the two innermost layers (layers 6 and 7) are fixed. The conjugate gradient algorithm described in Ref. 11 is used for the electronic energy minimization. In the spirit of the Car-Parrinello scheme,¹² it is combined with a similar algorithm for the ionic energy minimization. (The gradients of the total energy with respect to the ionic positions are of course the Hellmann-Feynman forces.) This simultaneous electronic and ionic energy minimization has considerable computational advantages over the standard approach to obtaining the electronic and equilibrium structures. We find that a complete geometry optimization requires only a factor of 3 times as much computational effort as an (electronic) energy minimization for a single fixed geometry.

Since the energy surface $E(x,y)$ must have the same symmetry as the reconstructed crystal surface, we need only carry out calculations for positions of the adatom in the irreducible part of the surface cell. In agreement with the results obtained by Roberts and Needs¹³ we found that the $p(2 \times 2)$ alternating-buckled-dimer surface has the lowest energy. However, as in Ref. 13, the energy difference between this $p(2 \times 2)$ and the $p(2 \times 1)$ symmetric-dimer reconstruction was small (less than 0.1 eV/dimer). We therefore only carried out exhaustive calculations for positions (x,y) of the adatom in the irreducible quarter of the $p(2 \times 1)$ surface cell shown in Fig. 1. The complete energy surface was then generated by C_{2v} symmetry.¹⁴ [The validity of this approximation was checked by explicitly calculating a number of additional points in the $p(2 \times 2)$ cell. The energy difference between these points and the points generated by C_{2v} symmetry was less than 0.1 eV.] Figure 2 shows the energy surface obtained by interpolating the values of the total energy at the grid points with a Fourier series.¹⁵

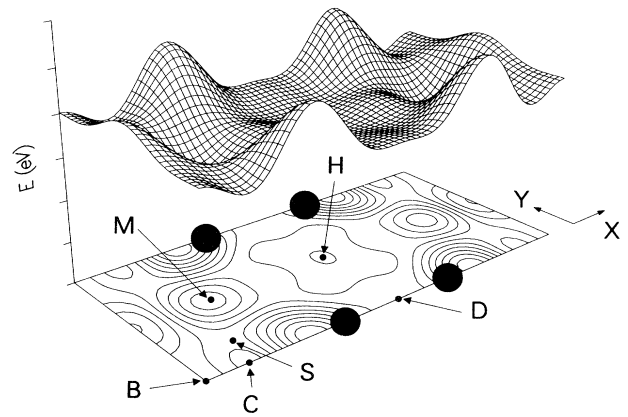


FIG. 2. Perspective view and contour plot of the total-energy surface $E(x,y)$. The $p(2 \times 1)$ unit cell corresponds to that shown in Fig. 1. The points indicated in the contour plot are the extremal points discussed in the text. The first contour is at 0.1 eV with respect to the absolute minimum (M) and the contour spacing is 0.2 eV. The interval on the vertical energy axis is 1 eV and the zero of energy is chosen arbitrarily. The x axis is chosen so as to pass through a dimer.

The interpolation based on this coarse grid was used to explore the topology of the energy surface. The energy minima were found by explicit energy minimization with respect to x and y . The saddle points were pinpointed by generating $E(x,y)$ on a finer grid once their approximate location was determined from the Fourier interpolation. In this way we confirmed that the topology of Fig. 2 is correct.

These results were obtained using a plane-wave energy cutoff of 8 Ry and a $p(\sqrt{8} \times \sqrt{8})R45^\circ$ Brillouin-zone sampling with two \mathbf{k} points. Increasing the cutoff to 12 Ry changed the energies relative to the minimum by 0.06 eV on the average. A similar change was found on increasing the number of \mathbf{k} points from two to four. Doubling the surface unit cell (to 16 surface atoms per cell) changed the energy differences by no more than 0.06 eV. Decreasing the number of layers in the slab from 12 to 10 resulted in changes of 0.02 eV in the total-energy differences, and increasing the vacuum spacing from 9.5 to 13.0 Å changed the results by less than 0.01 eV. From these studies, we estimate that convergence with respect to the size of the basis set and the supercell limits the accuracy of our results to around 0.1 eV. We have also performed a number of calculations keeping the substrate atoms fixed at the positions of the clean (reconstructed) Si(100) surface. From this we conclude that the effect of the substrate relaxation on total-energy differences is about 0.5 eV. Consequently, describing this relaxation properly is very important.

We can identify the binding position of the adatom from the absolute minimum (point M) on the interpolated total-energy surface given in Fig. 2. A more accurate binding geometry is obtained by minimizing the total en-

ergy with respect to all degrees of freedom, starting from a nearby grid point. The geometry of the resulting equilibrium binding configuration of adatom and substrate (shown in Fig. 3) may be understood in terms of the adatom making as many covalent bonds as possible without disrupting the underlying substrate. The long-bridge site (point *B* in Fig. 2), where the adatom connects two dimers in adjacent rows, might at first sight seem to be the most favorable, and has indeed been proposed as the binding site for Al and Ga adatoms.¹⁶ For Si adatoms, however, the adatom-dimer bonds in this geometry are too long (2.49 Å). The bonds of the dimers are stretched to 2.41 Å, whereas the bond length of dimers that do not bind to the adatom is 2.31 Å. The energy of this *B*-site geometry is 1.0 eV higher than that of the equilibrium binding geometry (*M* in Fig. 2). In the equilibrium geometry shown in Fig. 3, the adatom is bonded to two dimers which belong to the same dimer row. All bond lengths are ~ 2.35 Å. Although the distance of the adatom to the second-layer substrate atom is only 2.40 Å, the charge density only shows two directional bonds to the first-layer substrate atoms. The quasi-hexagonal site (*H* in Fig. 2) corresponds to a local minimum on the energy surface. The adatom at this site forms four long bonds of 2.48 Å to the substrate and stretches the dimer bonds to 2.42 Å. The total energy for this site is 0.25 eV higher than the absolute minimum so that at temperatures which are not too high, the equilibrium population of the site will not be significant.

If we describe the diffusion of an adatom on a surface within the framework of transition-state theory,¹⁷ it is necessary to determine the activation energy for a jump between two binding sites. Formally, one should locate the maximum energy along each possible path in the complete configuration space which connects the configurations of the two binding sites. The minimum energy among these maxima is the activation energy and the total-energy function then has a saddle point at the corresponding configuration. In practice, the search for the saddle point is limited to a physically reasonable portion of configuration space.¹⁸ In our case, we trace paths

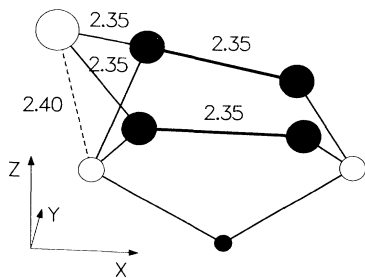


FIG. 3. Perspective view of the equilibrium binding configuration showing the first-, second-, and third-layer substrate atoms as in Fig. 1, and the bond lengths in angstroms. The adatom is shown as a large open circle.

which lie on the energy surface $E(x,y)$ by calculating E at intervals of 0.24 Å.

In general, the diffusion constant will be different for the two principal directions on the surface. (Even a relatively small difference in activation energies for jumps in these two directions can have a large effect on the anisotropy in the diffusion.) These principal directions on the Si(100) surface are along and perpendicular to the dimer rows, respectively. Consider Fig. 2; an adatom jumping along the dimer rows from the binding site in one cell to the binding site in an adjacent cell must cross the x axis (which goes through the two atoms of a dimer) at some point. Performing a total-energy minimization in which the adatom is constrained to lie on the x axis, we find two local minima on the x axis. At the first minimum (*D* in Fig. 2), whose energy is 0.6 eV higher than the energy of the absolute minimum (*M*), the adatom is positioned directly on top of a dimer. We verified by explicit calculation that there is a path connecting the absolute minima of two adjacent cells which passes through this point and on which this point is a maximum. This path runs from the *D* site to the local minimum at the *H* site and from there to the binding position. Consequently, this point represents a saddle-point configuration. The other path we consider passes through the second local minimum on the x axis (point *C* in Fig. 2), which is also a minimum in the y direction. If we trace a path from *C* to the absolute minimum, a saddle point (*S* in Fig. 2) is crossed whose energy is 0.8 eV. (We located this saddle point by a local search on a grid with a spacing of 0.24 Å. Furthermore, we were guided by the force on the adatom which is by construction equal to the gradient on our energy surface.) The activation energy for diffusion along the dimer rows is thus that of the first path, namely, 0.6 eV. In the same way, a point near the *B* site in Fig. 2 was established as the saddle-point configuration for diffusion perpendicular to the dimer rows. The associated activation energy is 1.0 eV.

As a result of this difference in activation energies the diffusion will be very anisotropic. For example, consider an STM experiment where the time between two observations is of the order of 10^2 sec. We can estimate the root-mean-square displacement at room temperature in this time to be $\sim 10^3$ Å along the dimer rows and less than 1 Å perpendicular to the dimer rows (using a typical value of 10^{13} Hz for the prefactor of the jump rate¹⁹). At room temperature, the adatoms will thus move exclusively *along* the dimer rows. In a number of experiments related to growth on the Si(100) surface, there have been speculations on the anisotropy of the diffusion of Si adatoms. The suggestion that the direction of easy diffusion is perpendicular to the dimer rows^{1,20} can clearly be ruled out from our calculations. The conclusion of Mo *et al.*² that the diffusion is nearly isotropic is not based on direct evidence such as the observation of diffusing atoms and is also contradicted by our calculations.

Making due allowance for the fact that a small uncertainty in the activation energy has a relatively large effect on the diffusion constant, we have found that individual Si atoms are mobile at room temperature. We believe that in experiments up until now, the time elapsed between deposition and observation was sufficient for the adatoms to migrate to a binding position at a step edge or an island. This is consistent with the fact that in the STM experiments so far no individual Si adatoms have been identified.¹⁻³ At this state it is not possible to assess in what way the anisotropic diffusion will influence growth on Si(100) surfaces. The statements about the importance of the anisotropic diffusion, which are based on Monte Carlo kinetics simulations, are contradictory.^{2,5} Diffusion is clearly one of the important issues, but a detailed study of growth requires knowledge of the energies associated with the nucleation process. The stable binding position of a single adatom, as obtained from the calculations, differs from a position which is required by epitaxial growth (such positions are the *D* or the *B* site; see Fig. 1). Furthermore, although at some points on the energy surface of Fig. 2 the reconstruction of the Si(100) surface is distorted, at no point are the dimer bonds actually broken. Thus an epitaxial layer cannot be constructed simply from individual adatoms. The details of the nucleation process remain a subject for later studies. Meanwhile, it is interesting to try to obtain direct experimental information on diffusing adatoms. From the activation energies which we have presented, it should be possible to observe one-dimensional diffusion of adatoms in STM experiments if the adatoms are deposited at temperatures of about 200 K.

Note added.—Recently, Dijkkamp, van Loenen, and Elswijk have performed an STM experiment in which one-dimensional diffusion on the Si(100) surface is observed.²¹

¹R. J. Hamers, U. K. Köhler, and J. E. Demuth, *Ultramicroscopy* **31**, 10 (1989); *J. Vac. Sci. Technol. A* **8**, 195 (1990).

²Y. W. Mo, B. S. Swartzentruber, R. Kariotis, M. B. Webb, and M. G. Lagally, *Phys. Rev. Lett.* **63**, 2393 (1989); *J. Vac. Sci. Technol. A* **8**, 201 (1990).

³A. J. Hoeven, J. M. Lenssinck, D. Dijkkamp, E. J. van Loenen, and J. Dieleman, *Phys. Rev. Lett.* **63**, 1830 (1989).

⁴E. J. van Loenen, H. B. Elswijk, A. J. Hoeven, D. Dijkkamp, J. M. Lenssinck and J. Dieleman, in *Kinetics of Ordering and Growth at Surfaces*, Proceedings of the NATO Advanced Research Workshop (Plenum, New York, 1989).

⁵A. Rockett, *Surf. Sci.* **227**, 208 (1990).

⁶For a review, see the article by F. Allen and E. Kasper, in *Silicon Molecular Beam Epitaxy*, edited by E. Kasper and J. C. Bean (CRC Press, Boca Raton, FL, 1988), Vol. I, p. 65, and references therein.

⁷S. C. Wang and G. Ehrlich, *Phys. Rev. Lett.* **62**, 2297 (1989); G. L. Kellogg and P. J. Feibelman, *Phys. Rev. Lett.* **64**, 3143 (1990); C. Chen and T. T. Tsong, *Phys. Rev. Lett.* **64**, 3147 (1990).

⁸G. B. Bachelet, D. R. Hamann, and M. Schlüter, *Phys. Rev. B* **26**, 4199 (1982).

⁹L. Kleinman and D. M. Bylander, *Phys. Rev. Lett.* **48**, 1425 (1982).

¹⁰The surface lattice which is generated by the $p(\sqrt{8} \times \sqrt{8})R45^\circ$ cell is frequently described as $c(4 \times 4)$.

¹¹I. Stich, R. Car, M. Parrinello, and S. Baroni, *Phys. Rev. B* **39**, 4997 (1989).

¹²R. Car and M. Parrinello, *Phys. Rev. Lett.* **55**, 2471 (1985).

¹³N. Roberts and R. J. Needs, *Surf. Sci.* **236**, 112 (1990).

¹⁴We stress that this approximation is only used to reduce the number of independent grid points (x, y). The geometry of the adatom and surface is not constrained in any way.

¹⁵C. G. van de Walle, Y. Bar-Yam, and S. T. Pantelides, *Phys. Rev. Lett.* **60**, 2761 (1988).

¹⁶I. P. Batra, *Phys. Rev. Lett.* **63**, 1704 (1989).

¹⁷G. Vineyard, *J. Phys. Chem. Solids* **3**, 121 (1957).

¹⁸C. H. Bennett, in *Diffusion in Solids*, edited by A. S. Nowick and J. J. Burton (Academic, New York, 1975), p. 73.

¹⁹The prefactor for the jump rate can be estimated from the energy surface $E(x, y)$ as in P. E. Blöchl, C. G. van de Walle, and S. T. Pantelides, *Phys. Rev. Lett.* **64**, 1401 (1990).

²⁰S. Stoyanov, *J. Cryst. Growth* **94**, 751 (1989).

²¹D. Dijkkamp, E. J. van Loenen, and H. B. Elswijk (to be published).